Synthesis and Mesomorphic Properties of Side-Chain Cholesteric Liquid-Crystalline Polymers Containing Menthyl Groups

Bing-Guang Du,[1] Jian-She Hu,[1] Bao-Yan Zhang,[1] Lin-Jiu Xiao,[2] Ke-Qi Wei[1]

[1]*Center for Molecular Science and Engineering, Northeastern University, Shenyang 110004, People's Republic of China*
[2]*Institute of Chemical Technology, Shenyang 110142, China, People's Republic of China*

Received 11 October 2005; accepted 13 December 2005
DOI 10.1002/app.23949
Published online in Wiley InterScience (www.interscience.wiley.com).

ABSTRACT: A series of new cholesteric liquid-crystalline polysiloxanes ($\mathbf{P_1}$–$\mathbf{P_5}$) derived from menthyl groups were synthesized. The chemical structures of the monomers and polymers were characterized with Fourier transform infrared, ^{1}H-NMR, ^{13}C-NMR, and elemental analyses. The mesomorphic properties and thermal behavior were investigated with differential scanning calorimetry, polarizing optical microscopy, thermogravimetric analysis, and X-ray diffraction measurements. The influence of the polymer structure on the thermal behavior was discussed. The monomer diosgeninyl 4-allyloxybenzoate exhibited a typical cholesteric oily-streak texture and a focal-conic texture. Polymers $\mathbf{P_1}$–$\mathbf{P_5}$ showed thermotropic liquid-crystalline properties. $\mathbf{P_1}$ displayed a smectic fan-shaped texture, $\mathbf{P_2}$–$\mathbf{P_5}$ showed a cholesteric Grandjean texture, and $\mathbf{P_6}$ and $\mathbf{P_7}$ did not show mesomorphic properties. The experimental results demonstrated that the glass-transition temperature and the clearing temperature decreased, and the mesomorphic properties weakened with an increasing concentration of menthyl units. Moreover, $\mathbf{P_1}$–$\mathbf{P_5}$ exhibited wide mesophase temperature ranges and high thermal stability. J Appl Polym Sci 102: 5559–5565, 2006

Key words: liquid-crystalline polymers (LCP); phase behavior; synthesis

INTRODUCTION

Cholesteric liquid-crystalline polymers (LCPs) have attracted considerable interest because of their unique optical properties, including selective reflection of light, thermochromism, and circular dichroism. This has led to advanced applications, such as nonlinear optical devices, full-color thermal imaging, and specific organic pigments.[1–7] For comblike polymers, the mesomorphic properties of side-chain LCPs mainly depend on the nature of the polymer backbone, the type of mesogen, the length of the flexible spacer, and the nature of the terminal groups.[8–11] The polymer backbones of side-chain LCPs are primarily polyacrylates, polymethacrylates, and polysiloxanes; however, polyacrylates and polymethacrylates, because of their backbones, show higher glass-transition temperatures (T_g's) and higher viscosities. For higher mobility of the mesophase and mesomorphic properties at moderate temperatures, a polysiloxane backbone and a flexible spacer are usually adopted. The cholesteric phase is formed by rodlike, chiral molecules responsible for the macroscopic alignment of the cholesteric domains. Depending on the chemical structures, it may be feasible to achieve a macroscopic alignment of the cholesteric domains. Recently, many novel side-chain cholesteric liquid-crystalline (LC) materials have been reported, and work continues in extending the range of these materials and exploring their application.[14–26]

In this study, a series of cholesteric LCPs derived from diosgeninyl 4-allyloxybenzoate ($\mathbf{M_1}$) and menthyl 4-(10-undecylen-1-yloxy)benzoate ($\mathbf{M_2}$) were synthesized and characterized. The mesomorphic properties and phase behavior of the monomers and polymers were investigated with differential scanning calorimetry (DSC), polarizing optical microscopy (POM), thermogravimetric analysis (TGA), and X-ray diffraction (XRD). The influence of the concentration of nonmesogenic chiral $\mathbf{M_2}$ units on the thermal behavior of LCPs is discussed in detail.

Correspondence to: B.-Y. Zhang (baoyanzhang@hotmail.com).
Contract grant sponsor: National Natural Science Fundamental Committee of China.
Contract grant sponsor: Specialized Research Fund for the Doctoral Program of Higher Education.
Contract grant sponsor: Natural Science Foundation of Liaoning Province.
Contract grant sponsor: Science and Technology Bureau of Shenyang.
Contract grant sponsor: China Postdoctoral Science Foundation.

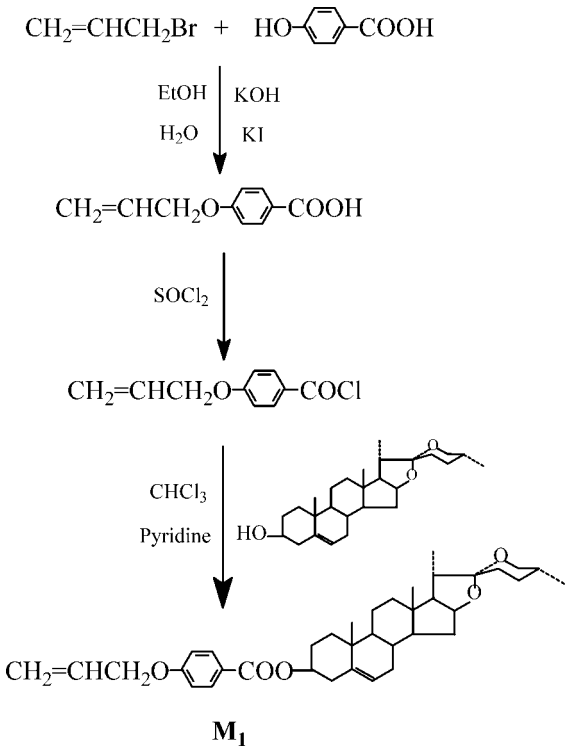

Scheme 1 Synthetic route of the LC monomer.

EXPERIMENTAL

Materials

Polymethylhydrosiloxane [PMHS; number-average molecular weight (M_n) = 700–800] was purchased from Jilin Chemical Industry Co. (Jilin, China). Diosgenin was purchased from Wuhan Ruixin Chemical Co. (Wuhan, China). Menthol was purchased from Shanghai Kabo Chemical Co. (Shanghai, China). Undecylenic acid was purchased from Beijing Jinlong Chemical Reagent Co., Ltd. (Beijing, China). The H_2PtCl_6 catalyst was obtained from Shenyang Chemical Reagent Co. The toluene used in the hydrosilylation reaction was purified by a treatment with $LiAlH_4$ and distilled before use. All solvents and reagents were purified by standard methods.

Characterization

Fourier transform infrared spectra were measured on a Spectrum One (B) spectrometer (PerkinElmer, Foster City, CA). ^{1}H-NMR spectra (300 MHz) and ^{13}C-NMR (75.4 MHz) spectra were obtained with a Gemini 300 spectrometer (Varian Associates, Palo Alto, CA). The elemental analyses (EAs) were carried out with a Vario EL III (Elementar, Germany). The optical rotations were obtained on a PerkinElmer 341 polarimeter. The phase-transition temperatures and thermodynamic parameters were determined with a DSC 204 (Netzsch, Wittelsbacherstr, Germany) equipped with a liquid-nitrogen cooling system. The heating and cooling rates were 10°C/min. The thermal stability of the polymers under nitrogen gas was measured with a Netzsch TGA 209C thermogravimetric analyzer. A DMRX POM instrument (Leica, Wetzlar, Germany) equipped with a THMSE-600 hot stage (Linkam, Surrey, England) was used under an atmosphere to observe the phase-transition temperatures and analyze the LC properties for the monomers and polymers through the observation of optical textures. XRD measurements were performed with nickel-filtered Cu Kα radiation with a DMAX-3A powder diffractometer (Rigaku, Tokyo, Japan).

Synthesis of the monomers

The synthetic route to the olefinic monomers is shown in Schemes 1 and 2. 4-Allyloxybenzoic acid (**1**) and 4-(10-undecylen-1-yloxy)benzoic acid (**2**) were prepared according to methods reported previously.[22,25]

M_1

M_1 was prepared according to procedures previously reported.[27]

Yield: 66%. mp: 182°C. $[\alpha]_D^{28}$: −43.5° (toluene). IR (KBr, cm^{-1}): 3074 (=C—H); 2944, 2830 (—CH_3, —CH_2—); 1713 (C=O); 1643 (C=C); 1606, 1455 (Ar—); 1249 (C—O—C). ^{1}H-NMR [$CDCl_3$, tetramethylsilane (TMS), δ, ppm]: 0.78–2.46 [m, 36H, diosgeninyl-*H*]; 3.34–3.52 (t, 3H, >C*H*O— and —O*CH*$_2$— in diosgeninyl); 4.38–4.81 (t, 3H, —ArCOOC*H*<, —C*H*$_2$OAr—); 5.26 (m, 2H, C*H*$_2$=CH—); 5.39 (m, 1H, =C*H*— in diosgeninyl), 6.04 (m, 1H, =C*H*—), 6.91–7.99 (m, 4H, Ar—*H*). ^{13}C-NMR ($CDCl_3$, TMS, δ ppm): 6.1, 16.5, 20.8, 21.3 (methyl-C); 21.5, 24.3, 26.7, 30.5, 31.7, 32.0, 32.5, 32.7, 39.6, 69.1, 75.4 (methylene-C); 30.1, 30.2, 36.4, 40.5, 42.3, 47.5, 68.6, 76.1 (tertiary C in diosgeninyl); 113.6, 131.1 (aromatic tertiary C); 35.5, 39.8, 111.9 (quaternary C in diosgeninyl); 123.2, 165.3 (aromatic quaternary C); 116.3 (CH_2=); 138.2 (=CH—); 121.9 (=CH— in diosgeninyl); 148.5 (>C= in diosge-

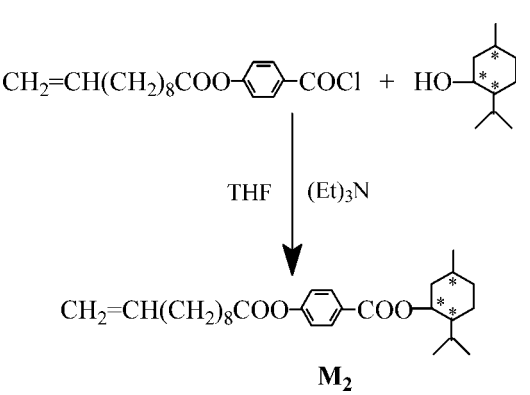

Scheme 2 Synthetic route of the chiral monomer.

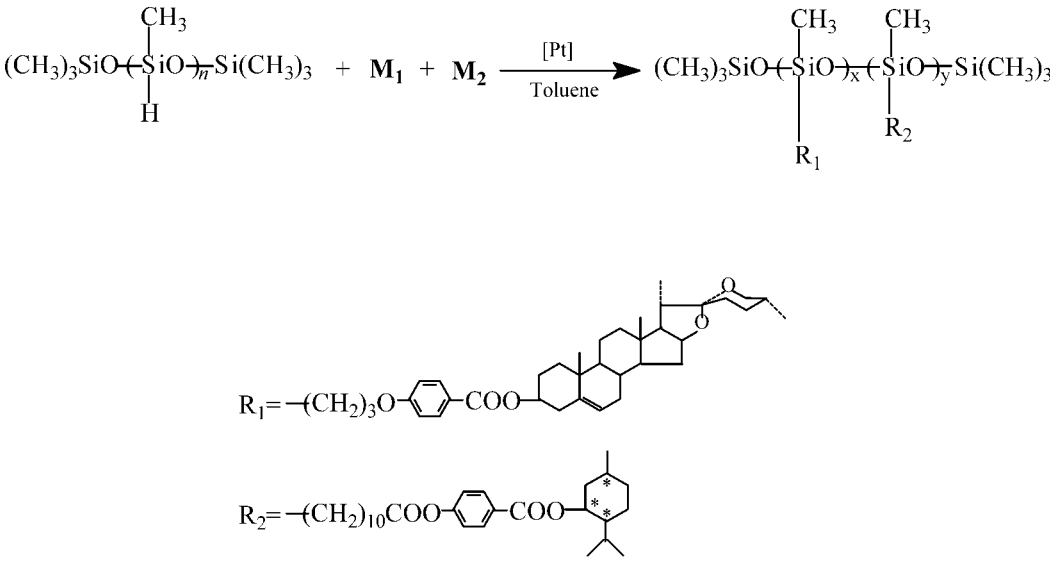

Scheme 3 Synthetic route of LCPs.

ninyl); 168.4 (C=O). ANAL. Calcd for $C_{37}H_{50}O_5$: C, 77.31%; H, 8.77%. Found: C, 77.15%; H, 8.91%.

M_2

Compound **2** (18.1 g, 0.06 mol) was reacted at 65°C with 35 mL of thionyl chloride containing a few drops of *N,N*-dimethylformamide for 7 h, and then the excess thionyl chloride was removed under reduced pressure to give the corresponding acid chloride. 4-(10-Undecylen-1-yloxy)benzoyl chloride that was obtained (16.1 g, 0.05 mol) was dissolved in 10 mL of tetrahydrofuran (THF) and then added dropwise to a stirred solution of menthol (7.8 g, 0.05 mol) in 30 mL of THF and 7 mL of triethylamine. After refluxing for 12 h, the reaction mixture was poured into much ice water. The crude product was obtained by filtration and washed with water. White crystals were obtained.

Yield: 61%. mp: 62°C. $[\alpha]_D^{28}$: −1.2° (toluene). IR (KBr, cm^{-1}): 3070 (=C—H); 2952, 2855 (—CH_3, —CH_2—); 1764, 1715 (C=O); 1640(C=C); 1603, 1510 (Ar—). ^{1}H-NMR ($CDCl_3$, TMS, δ ppm): 0.93–2.26 [m, 34H, —$(CH_2)_8$— and menthyl-*H*]; 4.09 (m, 1H, —ArCOOC*H*<); 4.98 (d, 2H, CH_2=CH—); 5.82 (m, 1H, =C*H*—); 7.15–7.99 (m, 4H, Ar—*H*). ^{13}C-NMR ($CDCl_3$, TMS, δ, ppm): 18.5, 19.3 (methyl-C); 24.8, 29.5, 30.0, 30.5, 33.5, 34.1 (aliphatic methylene-C); 19.8, 32.8, 37.1 (methylene-C in menthyl); 22.4, 24.9, 42.5, 68.2 (tertiary C in menthyl); 120.9, 130.4 (aromatic tertiary C); 127.4, 158.1 (aromatic quaternary C); 112.8 (CH_2=); 141.5 (=CH—); 166.3, 170.4 (C=O). ANAL. Calcd for $C_{28}H_{42}O_4$: C, 75.98%; H, 9.56%. Found: C, 75.25%; H, 9.48%.

Synthesis of the polymers

The synthesis of polymers $\mathbf{P_1}$–$\mathbf{P_7}$ is shown in Scheme 3. $\mathbf{P_1}$–$\mathbf{P_7}$ were synthesized by the same methods; the synthesis of $\mathbf{P_3}$ is described as an example. $\mathbf{M_1}$, $\mathbf{M_2}$, and PMHS (Table I) were dissolved in dried toluene. The reaction mixture was heated to 65°C under nitrogen, and then 2 mL of a THF solution of the H_2PtCl_6 catalyst (5 mg/mL) was injected with a

TABLE I
Polymerization, Yield and Solubility

Polymer	Feed (mmol) $\mathbf{M_1}$	Feed (mmol) $\mathbf{M_2}$	$\mathbf{M_2}$[a] (mol %)	Yield (%)	$M_n \times 10^{-3}$	Solubility in toluene[b]
$\mathbf{P_1}$	7.00	0.00	0	88	4.62	+
$\mathbf{P_2}$	6.65	0.35	5	91	4.51	+
$\mathbf{P_3}$	6.30	0.70	10	86	4.47	+
$\mathbf{P_4}$	5.60	1.40	20	85	4.35	+
$\mathbf{P_5}$	3.00	3.50	50	90	3.82	+
$\mathbf{P_6}$	1.40	5.60	80	87	3.77	+
$\mathbf{P_7}$	0.00	7.00	100	89	3.63	+

[a] Molar fraction of $\mathbf{M_2}$ based on $\mathbf{M_1}$ + $\mathbf{M_2}$.
[b] + = soluble.

TABLE II
Phase-Transition Temperatures of the Monomers

Monomer	Transition temperature (°C)[a]
$\mathbf{M_1}$	Heating: K 182.3 (36.5) Ch 207.6 (1.2) I Cooling: I 205.4 (2.6) Ch 158.9 (29.7) K
$\mathbf{M_2}$	Heating: K 62.4 (23.7) I Cooling: I 50.1 (20.7) K

[a] The corresponding enthalpy changes are shown in parentheses (J/g). K = solid; Ch = cholesteric; I = isotropic.

syringe. The hydrosilylation reaction, monitored via the Si—H stretch intensity, was completed within 30 h, as indicated by IR. $\mathbf{P_3}$ was obtained and purified by several reprecipitations from toluene solutions into methanol and then was dried *in vacuo*.

IR (KBr): 2951–2871 (—CH_3, —CH_2—); 1764, 1714 (C=O); 1605, 1501 (Ar); 1300–1000 cm^{-1} (Si—O—Si, C—Si, and C—O—C).

RESULTS AND DISCUSSION

Synthesis

The target monomers and polymers were synthesized according to Schemes 1–3. $\mathbf{M_2}$ was obtained through the reaction of 4-(10-undecylen-1-yloxy)benzoyl chloride with menthol in THF in the presence of triethylamine. The structure of $\mathbf{M_2}$ was characterized with IR, ^{1}H-NMR, and ^{13}C-NMR spectra. IR spectra of $\mathbf{M_2}$ confirmed the presence of characteristic bands at 1764 and 1715 cm^{-1} attributed to the ester C=O stretching band, at 1640 cm^{-1} attributed to the C=C stretching band, and at 1603 and 1510 cm^{-1} attributed to the aromatic stretching band. ^{1}H-NMR spectra of $\mathbf{M_2}$ showed multiplets at 7.99–7.15, 5.82–4.98, and 4.09–0.93 ppm corresponding to aromatic protons, olefinic protons, and methenyl, methylene, and methyl protons, respectively. The spectra of $\mathbf{M_2}$ suggested that the purity was high, and this was confirmed by EA.

The polymers were prepared by hydrosilylation reactions. IR spectra of the polymers showed the complete disappearance of the Si—H stretching band at 2166 cm^{-1}. Characteristic Si—O—Si stretching bands appeared at 1300–1000 cm^{-1}. The polymerization, yields, and solubility of the polymers are summarized in Table I. All polymers were soluble in toluene and xylene.

Mesomorphic properties

The mesomorphic properties and thermal stability of the monomers and polymers were investigated with DSC, POM, TGA, and XRD. The phase-transition temperatures and corresponding enthalpy changes of $\mathbf{M_1}$, $\mathbf{M_2}$, and $\mathbf{P_1}$–$\mathbf{P_7}$ are summarized in Tables II and III. The phase-transition temperatures determined by DSC were consistent with POM observation results.

Monomer $\mathbf{M_1}$ showed a melting transition at 182.3°C and a cholesteric–isotropic phase transition at 207.6°C. In cooling scans, an isotropic–cholesteric phase transition appeared at 205.4°C, and crystallization appeared at 158.9°C. POM results showed that $\mathbf{M_1}$ exhibited an enantiotropic, thermotropic cholesteric phase. It displayed a typical cholesteric oily-streak texture and a focal-conic texture upon heating and cooling cycles. The optical textures of $\mathbf{M_1}$ are shown in Figure 1(a,b). However, $\mathbf{M_2}$ showed only a melting transition or a crystallization transition on DSC curves; this was consistent with the POM results. It indicated that $\mathbf{M_2}$ was a nonmesogenic compound.

DSC thermograms of $\mathbf{P_1}$–$\mathbf{P_5}$ displayed a glass transition at a low temperature and an LC–isotropic phase transition at a high temperature. However, DSC curves of $\mathbf{P_6}$ and $\mathbf{P_7}$ showed only a glass transition and no LC–isotropic phase transition. This indicated that the mesomorphic properties began to weaken and gradually disappeared when the concentration of nonmesogenic units of $\mathbf{M_2}$ was greater than 50 mol %. The POM results showed that polymers $\mathbf{P_1}$–$\mathbf{P_5}$ exhibited thermotropic LC properties. $\mathbf{P_1}$ exhibited a smectic fan-shaped texture.[27] $\mathbf{P_2}$–$\mathbf{P_5}$ exhibited a cholesteric Grandjean texture. This indicated that the introduction of the chiral menthyl unit into the polymer could induce a cholesteric phase. However, $\mathbf{P_6}$ and $\mathbf{P_7}$ did not show any other texture; this was consistent with the results obtained by DSC. The optical textures of $\mathbf{P_1}$ and $\mathbf{P_4}$ are shown in Figure 2(a–c).

In general, the thermal properties of side-chain LCPs are affected by the polymer backbone, the length of the flexible spacer, the bulk of the side groups, and the copolymer composition. For side-chain LCPs, the bulky side groups impose additional constraints on the motion of chain segments because of the steric hindrance effect and cause an increase in T_g. However, T_g is also affected by the length of the flexible spacer of side groups, similarly to the plasticization effect, which can make T_g fall. Figure 3 shows the influence

TABLE III
LC Properties of the Polymers

Polymer	T_g (°C)	T_i (°C)	ΔT[a]	T_d (°C)[b]	LC phase[c]
$\mathbf{P_1}$	118.4	300.7	182.3	323.6	S_A
$\mathbf{P_2}$	115.5	295.3	179.8	320.5	Ch
$\mathbf{P_3}$	113.9	290.6	176.7	316.4	Ch
$\mathbf{P_4}$	97.1	283.2	186.1	305.4	Ch
$\mathbf{P_5}$	64.7	272.0	213.8	292.2	Ch
$\mathbf{P_6}$	22.3	—	—	284.9	—
$\mathbf{P_7}$	9.7	—	—	295.0	—

[a] Mesophase temperature range ($T_i - T_g$).
[b] Temperature at which the 5% weight loss occurred.
[c] S_A = smectic A; Ch = cholesteric.

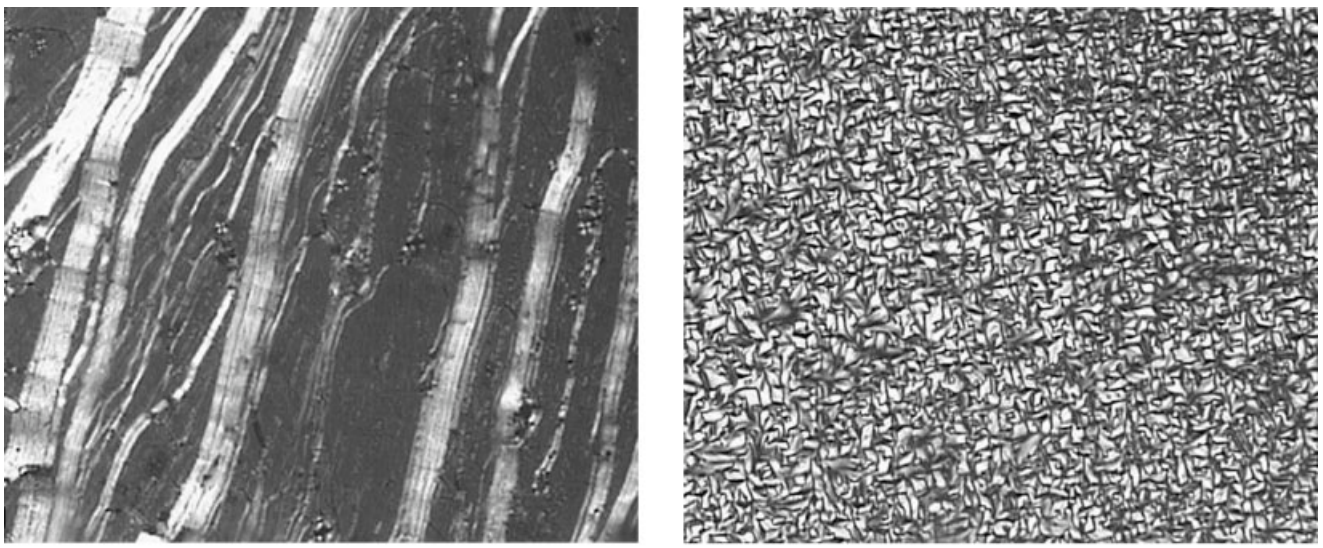

Figure 1 Optical textures of $\mathbf{M_1}$ (200×): (a) a cholesteric oily-streak texture on heating to 196°C and (b) a cholesteric focal-conic texture on cooling to 178°C.

of the copolymer composition on the thermal behavior of the polymers. As shown in Table III, T_g decreased from 118.4°C for $\mathbf{P_1}$ to 9.7°C for $\mathbf{P_7}$ when the concentration of menthyl units of $\mathbf{M_2}$ increased from 0 to 100%. The reasons were that (1) the content of bulky diosgeninyl groups decreased and (2) the plasticization effect of the flexible spacer of the menthyl groups increased. The two effects could make T_g decrease.

Along with T_g, the clearing temperature (T_i) was an important parameter of the LCPs. The copolymer composition affected T_i of the LCPs in two ways: (1) the flexible spacer of the menthyl units of $\mathbf{M_2}$ acted as a diluent in the polymer, causing a decrease in T_i, and (2) the introduction of the nonmesogenic $\mathbf{M_2}$ units into the polymer discouraged the orientation and formation of mesogenic molecules. According to Table III, T_i decreased from 300.7°C for $\mathbf{P_1}$ to 272.0°C for $\mathbf{P_5}$ when the concentration of menthyl units of $\mathbf{M_2}$ increased from 0 to 50 mol %. The mesomorphic properties of the polymers disappeared when the concentration of nonmesogenic units of $\mathbf{M_2}$ became greater than 50%. In addition, $\mathbf{P_1}$–$\mathbf{P_5}$ displayed a wider mesophase temperature range. Comparing the phase-transition temperatures of the polymers, we found that a flexible

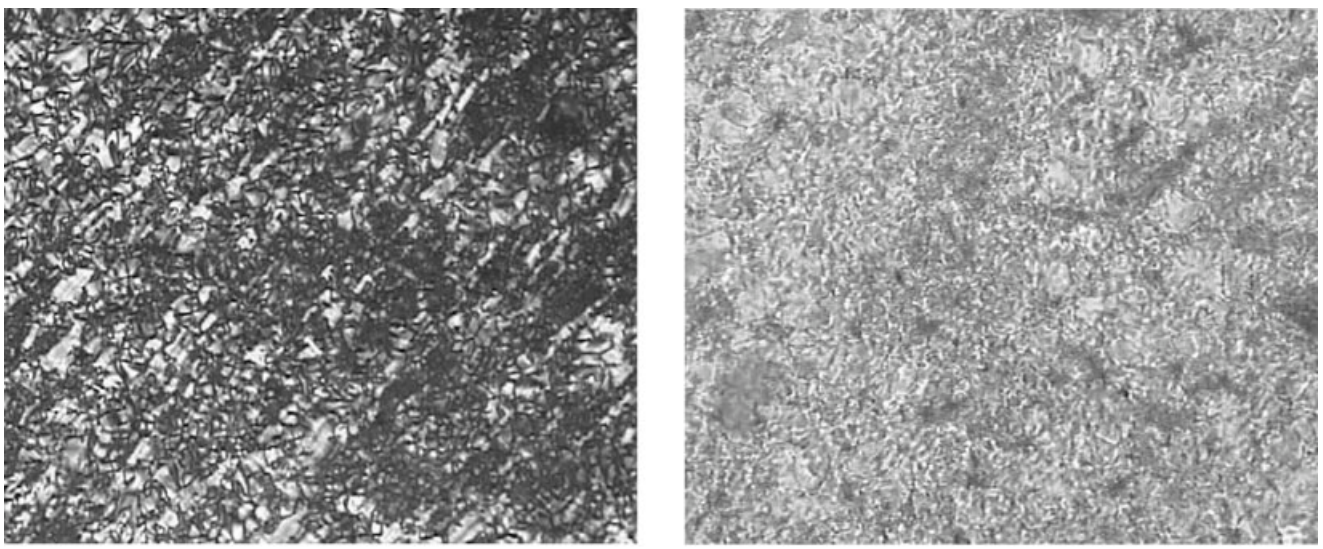

Figure 2 Optical textures of the polymers (200×): (a) the smectic fan-shaped texture of $\mathbf{P_1}$ at 246°C with annealing for 3 h and (b) the cholesteric Grandjean texture of $\mathbf{P_4}$ at 258°C.

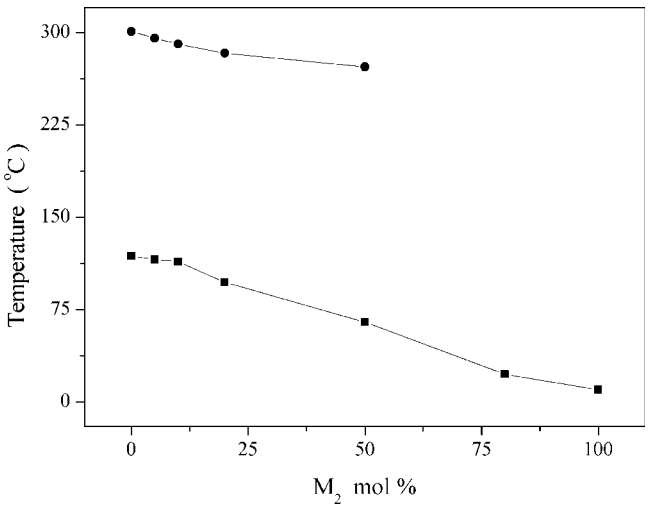

Figure 3 Effect of the $\mathbf{M_2}$ concentration on the phase-transition temperatures of the polymers.

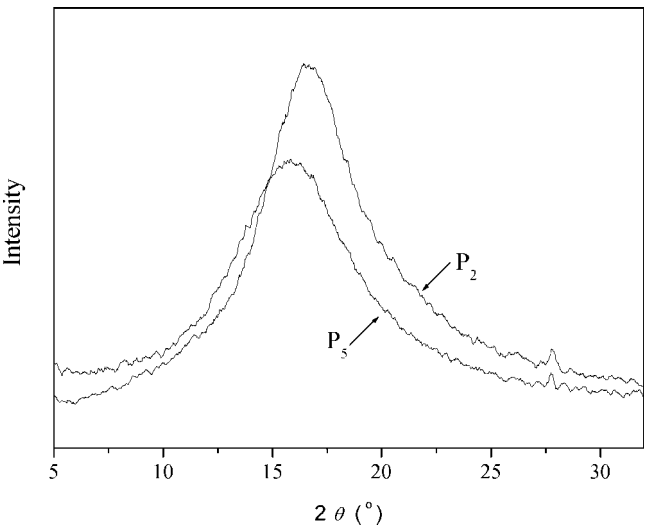

Figure 5 XRD patterns of $\mathbf{P_2}$ and $\mathbf{P_5}$.

polymer backbone and a long, flexible spacer tended to produce a low T_g and a wide mesophase temperature range.

The thermal stability of the polymers was detected with TGA. The corresponding data are shown in Table III. Figure 4 shows representative TGA curves of $\mathbf{P_2}$ and $\mathbf{P_5}$ as examples. The TGA results showed that the temperatures at which 5% weight losses occurred were greater than 280°C for $\mathbf{P_1}$–$\mathbf{P_7}$; this demonstrated that the synthesized polymers had higher thermal stability.

XRD studies were carried out to obtain more detailed information on the LC phase structure. In general, a sharp and strong peak at a low angle ($1° < 2\theta < 4°$) in small-angle X-ray scattering (SAXS) curves and a strong, broad peak associated with lateral packing at about $2\theta = 20°$ in wide-angle XRD curves could be observed for a smectic structure; no peak appeared in SAXS curves and a broad peak occurred at $2\theta = 16$–$18°$ for a cholesteric structure. Representative XRD curves of $\mathbf{P_2}$ and $\mathbf{P_5}$ are shown Figure 5. An XRD study of $\mathbf{P_1}$ can be found in the reported literature.[27] For $\mathbf{P_2}$–$\mathbf{P_5}$, a strong small-angle reflection was not observed, and a broad peak appeared at $2\theta = 16.0$–$16.8°$. Therefore, the LC phase structure was confirmed by the optical textures and XRD results.

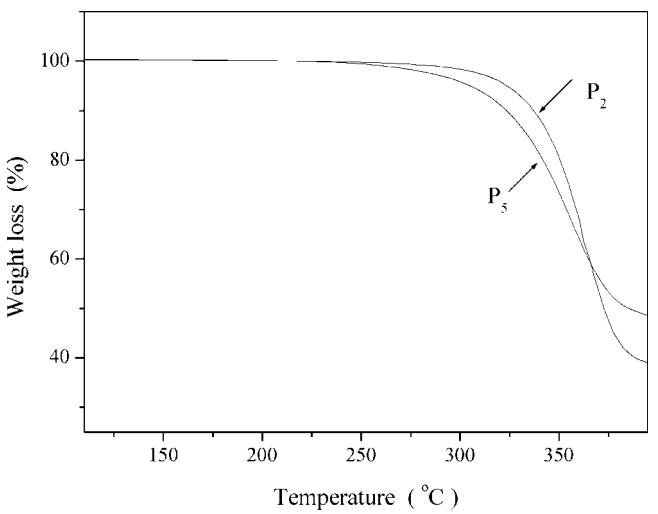

Figure 4 TGA curves of $\mathbf{P_2}$ and $\mathbf{P_5}$.

CONCLUSIONS

A series of new LCPs derived from diosgeninyl and menthyl groups were synthesized and characterized. Monomer $\mathbf{M_1}$ exhibited a typical cholesteric phase, and $\mathbf{M_2}$ was a chiral nonmesogenic monomer. Polymer $\mathbf{P_1}$ showed a smectic phase, $\mathbf{P_2}$–$\mathbf{P_5}$ showed a cholesteric phase, and $\mathbf{P_6}$ and $\mathbf{P_7}$ displayed no other texture. Moreover, the introduction of chiral menthyl units with longer, flexible spacers into LCPs could induce a cholesteric phase. The obtained LCPs exhibited wider mesophase temperature ranges and high thermal stability.

References

1. Broer, D. J.; Lub, J.; Mol, G. N. Nature 1995, 378, 467.
2. Bunning, T. J.; Kreuzer, F. H. Trends Polym Sci 1995, 3, 318.
3. Yang, D. K.; West, J. L.; Chien, L. C.; Doane, J. W. J Appl Phys 1994, 76, 1331.
4. Kricheldorf, H. R.; Sun, S. J.; Chen, C. P.; Chang, T. C. J Polym Sci Part A: Polym Chem 1997, 35, 1611.
5. Peter, P. M. Nature 1998, 391, 745.
6. Sapich, B.; Stumpe, J.; Krawinkel, T.; Kricheldorf, H. R. Macromolecules 1998, 31, 1016.
7. Sun, S. J.; Liao, L. C.; Chang, T. C. J Polym Sci Part A: Polym Chem 2000, 38, 1852.
8. Le Barney, P.; Dubois, J. C.; Friedrich, C.; Noel, C. Polym Bull 1986, 15, 341.

9. Hsu, C. S.; Percec, V. J Polym Sci Part A: Polym Chem 1989, 27, 453.
10. Hsiech, C. J.; Wu, S. H.; Hsiue, G. H.; Hsu, C. S. J Polym Sci Part A: Polym Chem 1994, 32, 1077.
11. Wu, Y. H.; Lu, Y. H.; Hsu, C. S. J Macromol Sci Pure Appl Chem 1995, 32, 1471.
12. Stohr, A.; Strohriegl, P. Macromol Chem Phys 1998, 199, 751.
13. Dierking, I.; Kosbar, L. L.; Held, G. A. Liq Cryst 1998, 24, 387.
14. Holter, D.; Frey, H.; Klee, J. E. Adv Mater 1998, 10, 864.
15. Maxein, G.; Mayer, S.; Zentel, R. Macromolecules 1999, 32, 5747.
16. Pfeuffer, T.; Strohriegl, P. Macromol Chem Phys 1999, 200, 2480.
17. Finkelmann, H.; Kim, S. T.; Munoz, A.; Taheri, B. Adv Mater 2001, 13, 1069.
18. Kim, S. T.; Finkelmann, H. Macromol Rapid Commun 2001, 22, 429.
19. Cicuta, P.; Tajbakhsh, A. R.; Terentjev, E. M. Phys Rev E 2002, 65, 051704.
20. Bermel, P. A.; Warner, M. Phys Rev E 2002, 65, 056614.
21. Hu, J. S.; Zhang, B. Y.; Jia, Y. G.; Chen, S. Macromolecules 2003, 36, 9060.
22. Hu, J. S.; Zhang, B. Y.; Liu, L. M.; Meng, F. B. J Appl Polym Sci 2003, 90, 3944.
23. Schmidtke, J.; Stille, W.; Finkelmann, H. Phys Rev Lett 2003, 90, 083902.
24. Hu, J. S.; Zhang, B. Y.; Guan, Y. J Polym Sci Part A: Polym Chem 2004, 42, 5262.
25. Hu, J. S.; Zhang, B. Y.; Yao, D. S.; Zhou, A. J. Liq Cryst 2004, 31, 393.
26. Hu, J. S.; Zhang, B. Y.; Zhou, A. J.; Dong, L. Y.; Zhao, Z. X. J Polym Sci Part A: Polym Chem 2004, 42, 5262.
27. Hu, J. S.; Zhang, B. Y.; Pan, W.; Li, Y. H. J Appl Polym Sci, 2006, 99, 2330.